Competition between molecular and dissociative adsorption of hydrogen on palladium clusters deposited on defective graphene

Alejandra Granja[1], Julio A. Alonso[1,2], Iván Cabria[1] and María J. López * [1]

[1]Departamento de Física Teórica, Atómica y Óptica, Universidad de Valladolid, 47011, Valladolid, Spain. Fax: +34-983-423013

[2]Donostia International Physics Center, 20080 San Sebastián, Spain

May 1, 2015

Abstract

The contribution of Pd doping to enhance the hydrogen storage capacity of porous carbon materials is investigated. Using the Density Functional Formalism, we have studied the competition between the molecular adsorption and the dissociative chemisorption of H_2 on Pd clusters anchored on graphene vacancies. The molecular adsorption of H_2 takes place with energies in the range of 0.7 - 0.3 eV for adsorption of one to six hydrogen molecules. Six molecules saturate the cluster, and additional hydrogen could only be adsorbed, with much smaller adsorption energies, at farther distances from the cluster. The dissociative chemisorption is the preferred adsorption channel from one to three hydrogen molecules, with adsorption energies in the range of 1.2 - 0.6 eV. After the first three molecules are dissociatively quemisorbed, three additional hydrogen molecules can be adsorbed

*Corresponding Author: E-mail: maria.lopez@fta.uva.es

non-dissociatively onto the Pd cluster with adsorption energies of 0.5 eV. The desorption of Pd-H complexes is prevented in all cases because the Pd clusters are firmly anchored to graphene vacancies. Our results are very promising and show that Pd clusters anchored on graphene vacancies retain their capacity to adsorb hydrogen and completely prevent the desorption of Pd-H complexes that would spoil the hydrogen releasing step of the cycle.

1 Introduction

The successful storage of hydrogen is a technological requirement to boost its use in electric cars powered by hydrogen fuel cells. However, the technological problem of storing 5.5 wt% hydrogen [1] at room temperature and moderate presures remains elusive and efforts are being invested in different directions. [2] The most promising technologies focus on the storage of hydrogen adsorbed in light solid materials, as porous carbons. These materials exhibit a reasonably high storage capacity [3,4] of about 6 wt% hydrogen at low temperatures (77 K) but their capacity drops dramatically to about 1 wt% hydrogen at room temperatures and moderate preasures, what is far from the technological requirement. Optimization of the size and shape of the pores yields some improvement [5,6] but the hydrogen storage capacity of these materials remains too low for practical application. The main difficulty arises from the small adsortion energy [7–10], below 100 meV, of hydrogen to the pore walls.

A recent experimental work by Contescu et al. [11] indicates an enhancement in the hydrogen storage capacity of porous carbon materials doped with palladium. It is, therefore, of great interest to understand and explain the mechanisms through which the Pd dopant contributes to the enhancement of the storage capacity of these materials. Recent computer simulations of the structure of nanoporous carbons performed by some of the authors [12] indicate that the walls of the pores are one atom thick planar or curved graphene-like layers containing defects. These results suggest that the pore walls of these materials can be modeled through a combination of pristine and defective graphene layers. Previous work has focused on the study of hydrogen adsorption on palladium atoms [13,14] and clusters [15] deposited on pristine graphene. We have shown [15]

that hydrogen adsorption takes place with enhanced adsorption energies, what seems to indicate a beneficial effect of palladium doping on the hydrogen storage capacity of porous carbons. However, since the bonding of the palladium clusters with the pristine graphene layer is relatively weak, of about 1 eV, desorption of Pd-H complexes competes with the desorption of hydrogen. Evidently, the desorption of hydrogen is a key step in the storage cycle and, therefore, the desorption of Pd-H complexes may inhibit the beneficial effect of Pd doping.

We have proposed[16], as a way to overcome this difficulty, to attach the Pd atoms and clusters to defects of the graphene layer, for instance to graphene vacancies. Pd atoms and clusters attach strongly to the vacancies, where they get firmly anchored to the graphene layer. Preliminar results on the adsorption of molecular hydrogen on a single Pd atom saturating a graphene vacancy[16] or a vacant site in the wall of a carbon nanotube[17], CNT, were quite promising. In this paper we have investigated the effect that anchoring small Pd clusters on graphene vacancies has on the adsorption/desorption of molecular hydrogen. This effect cannot be inferred from previous studies on pristine graphene. We have performed simulations, using the Density Functional Formalism, investigating the different adsorption channels, molecular and dissociative, of hydrogen on Pd clusters anchored on graphene vacancies, and the competion between those channels as a function of the number of adsorbed molecules. We have also studied the desorption step and the competition between desorption of hydrogen and desorption of Pd-H complexes. In Section II we present the key features of the Density Functional Formalism used in our computer simulations. Section III presents the results and we finish with some Conclusions in Section IV.

2 Theoretical Model

We have investigated the adsorption of hydrogen on a Pd_6 cluster anchored on a graphene vacancy using the Density Functional Formalism (DFT). The graphene layer is considered here as a model of the graphitic walls of nanoporous carbon materials, and the vacancies simulate defects of the walls. As we have shown in previous works[15,18],

palladium exhibits a strong tendency to aggregate and form three dimensional clusters on the surface of graphene. The clusters grow preferentially in the neighborhood of vacancies of the graphene layer, where they attach strongly. The DFT calculations have been performed with the DACAPO code[19]. The code implements the supercell methodology. The graphene layer is represented by a supercell containing 5×5 hexagonal unit cells, each of which contains two C atoms (see Fig.1). Thus the supercell size in the X direction is 12.33 Å. In the Z direction the supercell is taken large enough (14 Å) to avoid interactions between the images of the graphene layer in different supercells. The interactions of the valence electrons with the nuclear cores are described through Vanderbilt ultrasoft pseudopotentials[20]. A basis set of plane waves is used to expand the wave functions and the electronic density, with cutoff values of 350 eV and 1000 eV, respectively, for good convergence. We have considered four k points in the first Brillouin zone, following the Monkhorst-Pack scheme[21]. Since the supercells used in the calculations are quite large, this selection is sufficient to guarantee convergence in the cohesive energies better than 10 meV. The generalized gradient approximation of Perdew and Wang (GGA-PW91)[22] for the exchange-correlation functional is employed. An extensive search on the possible adsorption sites of the hydrogen molecules and of the hydrogen atoms of the dissociated molecule on the Pd_6 cluster has been performed. The search included the adsorption of hydrogen molecules and of hydrogen atoms on the vertices, edges and faces of the Pd_6 cluster. Then, all the structures, the graphene layer with the vacant site, the Pd_6 on the grahene monovacancy and the molecular and dissociated hydrogen adsorbed on the supported palladium clusters, have been fully optimized until the forces acting on all the atoms were smaller than 0.05 eV/Å.

3 Results

We have investigated the mechanisms of adsorption of Hydrogen on Pd_6 clusters bound to a graphene vacancy. Pd_6 clusters are taken as representatives for clusters in the small size range. The lowest energy octahedral, OCT, structure of free Pd_6 clusters experi-

Figure 1: Top and side views of the octahedral structure, OCT, and the icosahedral-type structure, ICO, of Pd_6 adsorbed on a graphene vacancy. The OCT structure binds to the graphene vacancy with an energy of 5.62 eV. The adsorbed ICO structure is 0.11 eV higher in energy than the OCT structure.

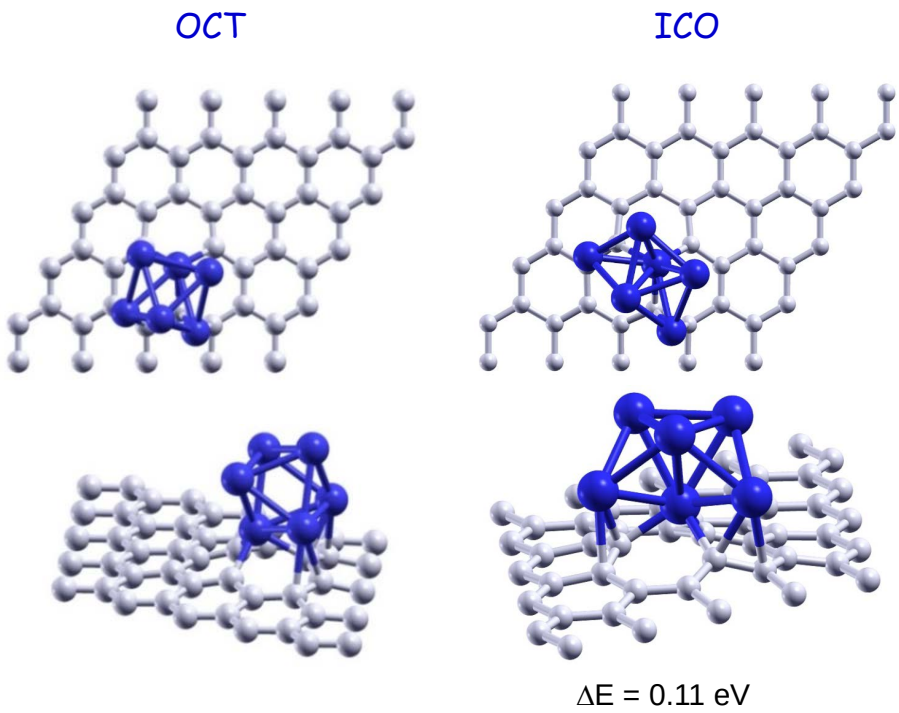

ences only a minor distortion upon deposition on a graphene layer with a vacancy, although it adsorbes with a substantial energy of 5.62 eV (see Fig.1). Pd_6 rests supported on one of its triangular faces. One of the Pd atoms of this face is sitting above the center of the vacancy, saturating the dangling bonds of the three C atoms around the vacant site. The other two Pd atoms are above two C–C bonds around the vacancy. The graphene layer distorts about the vacancy and the adsorbed Pd cluster. The C atoms in direct contact with the Pd-saturated vacancy get out of plane (in the direction of the Pd cluster) about 0.5-0.7 Å and the next shell of C atoms (counted from the vacancy) about 0.3-0.4 Å. The magnetic moment $\mu = 2\mu_B$ of the free Pd_6 cluster is quenched down to zero upon adsorption on the vacancy. This is in contrast with Pd_6 deposited on pristine graphene, that retains the magnetic moment of the free cluster. Molecular hydrogen may adsorb on the Pd_6 clusters anchored on graphene vacancies following two adsorption modes: i) molecular adsorption, in which the molecule is slightly activated

but the hydrogen atoms remain bound to each other and ii) dissociative adsorption, in which the molecule is broken and each hydrogen atom chemisorbs independently to the Pd cluster. These two adsorption modes were also found for hydrogen adsorption on palladium clusters supported on pristine graphene. We have studied in detail the competition between the two adsorption channels for palladium clusters anchored to a graphene vacancy as a function of the hydrogen content, that is, as additional hydrogen molecules adsorb into the clusters. The adsorption energies of the succesively attached hydrogen molecules to the Pd clusters are defined as

$$E_{ad}^{nth}(\mathrm{H_2}) = E[(n-1)\mathrm{H_2} + \mathrm{Pd_6} \text{ on } \mathrm{G_{vac}}] + E(\mathrm{H_2}) - E[n\mathrm{H_2} + \mathrm{Pd_6} \text{ on } \mathrm{G_{vac}}] \ , \quad (1)$$

where $E[n\mathrm{H_2} + \mathrm{Pd_6} \text{ on } \mathrm{G_{vac}}]$ is the energy of the system with n adsorbed hydrogen molecules, $E[(n-1)\mathrm{H_2} + \mathrm{Pd_6} \text{ on } \mathrm{G_{vac}}]$ is the energy of the system with $n-1$ adsorbed molecules, and $E(\mathrm{H_2})$ is the energy of a free hydrogen molecule. Clearly, $E_{ad}^{nth}(\mathrm{H_2})$ gives the adsorption energy for the nth hydrogen molecule adsorbing on a palladium cluster with $n-1$ adsorbed hydrogen molecules. This definition is valid for molecular adsorption and dissociative chemisorption, and, in each case, the configuration of the system with $n-1$ adsorbed molecules and the adsorption channel of the nth hydrogen molecule will be indicated.

3.1 Molecular adsorption of Hydrogen

The preferred site for the molecular adsorption of H_2 is on top of one of the Pd atoms which is not in direct contact with the graphene surface. The same behaviour was found for hydrogen adsorption on Pd_6 deposited on pristine graphene. The adsorption energy is 0.74 eV, somewhat higher than the adsorption energy, 0.56 eV, on Pd_6 supported on pristine graphene. The hydrogen molecule is slightly activated, the H–H distance becomes 0.86 Å. A little smaller activation, with H–H distances of 0.79-0.80 Å, is found for hydrogen molecules adsorbed on single Pd atoms saturating graphene or CNTs vacancies.[16,17] The H–H distance of the free H_2 molecule is 0.75 Å. The H–H bond is weakened but not broken. One hydrogen molecule can adsorb on top of any of

the Pd atoms of the cluster, except on top the Pd atom which is saturating the vacancy. The adsorption energies are quite similar, about 0.7 eV, for the three Pd atoms which are not in direct contact with the graphene layer, and are substantially reduced to 0.3 - 0.4 eV for the two Pd atoms directly in contact with the graphene surface.

Figure 2 shows the structures of the successive adsorption of molecular hydrogen on the OCT structure of Pd_6 anchored on a graphene vacancy. With a first molecule adsorbed, a second hydrogen molecule adsorbs preferentially on top of a different Pd atom, with a practically identical adsorption energy, 0.73 eV. Adsorption of a second molecule on top of the same Pd atom as the first one leads to a smaller adsorption energy of 0.44 eV. A somewhat lower adsorption energy, 0.53 eV, than the first two molecules is found for adsorption of the third hydrogen molecule on top of the remaining Pd atom which is not in direct contact with the graphene surface. On the other hand, adsorption on one of the occupied vertices leads a smaller adsorption energy, 0.40 eV. A fourth and a fifth hydrogen molecules can still be adsorbed on the two Pd atoms which are not occupied by previous hydrogen molecules, the two Pd atoms supported on the graphene layer, with adsorption energies of 0.47 and 0.34 eV respectively. However the fourth molecule has a slighty higher adsorption energy, 0.50 eV, for adsorption on one of the vertices which is not in direct contact with the graphene surface, although it is already occupied by another H_2 molecule. Then the fith molecule adsorbes on one of the Pd atoms in contact with the graphene surface with an energy of 0.36 eV, and a sixth molecule may adsorb in the remaining Pd atom in contact with graphene with an energy of 0.34 eV. All these results are summarized in Table 1. The distance between the hydrogen molecules and the corresponding Pd atoms where they are attached is quite constant, about 1.7-1.8 Å, for all the hydrogen molecules for adsorption between one and six molecules onto the Pd_6 cluster supported on the graphene vacancy. This distance is about 10% smaller than the distance of 2.0 Å between the hydrogen molecule and a single Pd atom saturating a graphene[16] or a CNT[17] vacancy. This indicates a stronger interaction of the hydrogen molecules with the Pd clusters than with the Pd atoms saturating carbon vacancies.

Direct adsorption of six hydrogen molecules seems to be the saturation limit on

Figure 2: Top and side views of successive molecular adsorption of hydrogen on the OCT structure of Pd_6 anchored on a graphene vacancy. The reported energies are the adsorption energies of the last hydrogen molecule calculated using Eq.1.

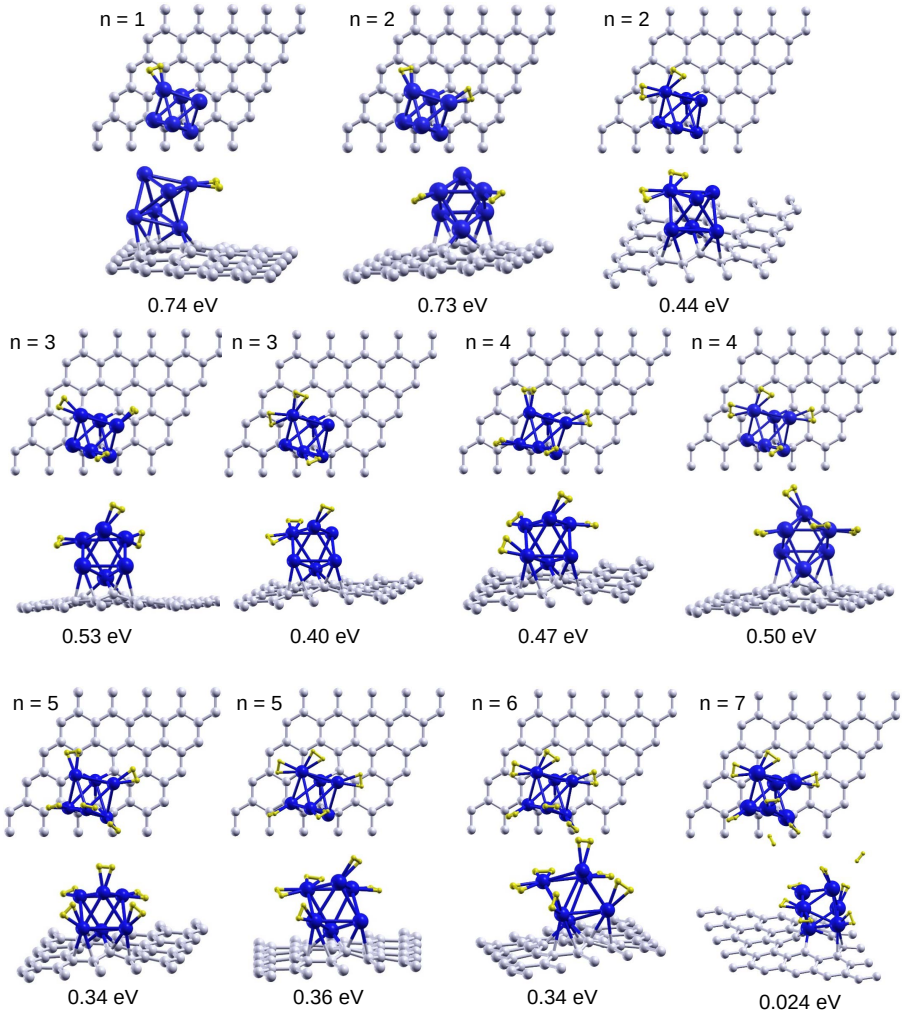

Pd_6 anchored on a vacancy. Because of the steric effects produced by the presence of the supporting graphene layer and by the previously bound hydrogen molecules, the seventh molecule cannot attach directly to the Pd cluster. This molecule will begin forming a second hydrogen shell around de Pd cluster, at a substantially longer distance, 3.2 Å, than the hydrogen molecules of the first layer, and with a quite small adsorption energy of the order of a few tens of meV. This adsorption strength is similar to that found for the second hydrogen layer covering pure carbon nanotubes[23]. We are not investigating this second layer because molecules having so small adsorption energies are not relevant for hydrogen storage at normal temperatures.

3.2 Dissociative Chemisorption of Hydrogen

The dissociative chemisorption channel is preferred over the molecular adsorption of hydrogen. The hydrogen molecule dissociates and the two hydrogen atoms adsorb on a face and an edge of the octahedron, respectively. The chemisorption energy of 1.03 eV is substantially larger than the molecular adsorption energy. The adsorption of the hydrogen atoms on two faces of the octahedron is slightly less stable, by only 0.05 eV (see Fig.3). Those structures, however, do not correspond to the lowest energy configuration. The dissociative chemisorption of hydrogen induces a structural transition in the palladium cluster from the octahedral structure to the structure of an incomplete pentagonal bipyramid in which one of the atoms of the pentagonal base is missing. One of the apex atoms of the bipyramid saturates the vacant site of graphene and the two base Pd atoms next to the empty base position attach to two C–C bonds, respectively, around the vacancy. We will refer this Pd_6 structure as ICO structure, because it can be viewed as part of an icosahedron (see Fig.1). We find a distortion of the graphene layer around the ICO structure of Pd_6 similar to that about the OCT structure. The ICO structure of the free Pd_6 cluster has a cohesive energy 0.29 eV lower (less stable) than the octahedral structure. Upon adsorption on a graphene vacancy the ICO structure gains some stability but it is still 0.11 eV less stable than the supported octahedron. It is the dissociative adsorption of hydrogen that prompts the structural change. The two hydrogen atoms attach to the two non-adjacent triangular faces at the side of the

Figure 3: Top and side views of the dissociative chemisorption of one hydrogen molecule on the OCT and ICO structures of Pd_6 anchored on a graphene vacancy. The reported energies are the adsorption energies calculated using Eq.1 for $n = 1$.

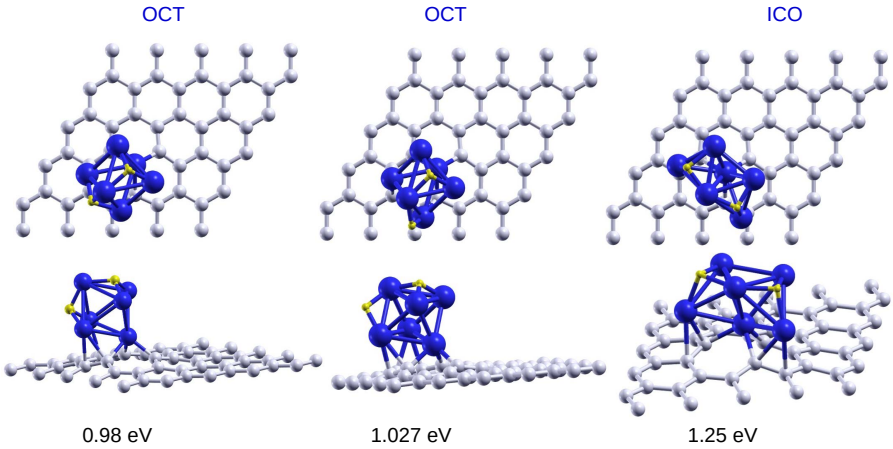

bipyramid whose apex atom is not the one saturating the vacancy (upper side of the bipyramid, for further reference). The hydrogen chemisorption energy, 1.25 eV per molecule, is 0.22 eV higher than the adsorption energy of the dissocciated molecule on the octahedral structure. The chemisorbed structures are shown in Fig.3. The dissociative chemisorption of hydrogen is also the preferred adsorption channel on Pd_6 supported on pristine graphene, with an energy of 1.30 eV. However, in this case the chemisorption of hydrogen does not induce a structural change in the Pd cluster.

3.3 Competition between dissociative chemisorption and molecular adsorption of Hydrogen

We have investigated the adsorption of several hydrogen molecules, and the competition between the dissociative chemisorption and the molecular adsorption. We start with the lowest energy ICO structure of Pd_6 supported on a graphene vacancy with one dissociatively chemisorbed hydrogen molecule, and investigate the adsorption of additional molecules. The structures are shown in Fig.4. A second hydrogen molecule adsorbs preferentially on the upper side of the bipyramid following also the dissociative chemisorption channel, with an adsorption energy of 0.90 eV. This energy is reduced a

bit with respect to the chemisorption of the first molecule. One of the hydrogen atoms becomes attached to the remaining face of the upper side of the bipyramid, and the second atom to one Pd–Pd bond of the bipyramid base, and one of the previously attached H atoms moves a little from a face position to above a Pd-Pd bond. This molecule may also attach as a nondissociated molecule on top of one of the Pd atoms of the base not in direct contact with the graphene layer, with almost the same energy of 0.87 eV. For adsorption of a third molecule, the two adsorption channels are also almost degenerate in energy. The adsorption energies of a third molecule on Pd_6 with two dissociated hydrogen molecules are 0.61 eV (molecular adsorption) and 0.58 eV (chemisorption). The dissociative channel is only 30 meV less stable than the molecular channel, that is within the limits of accuracy of our calculations. The dissociative chemisorption of the third molecule changes the adsorption site of one H atom, pushing it out of face. Then, finally only one H atom is attached to a face and the remaining H atoms attach to different Pd–Pd bonds. A forth molecule can not dissociate on Pd_6 with three dissociated hydrogen molecules. The adsorption energy is negative, -0.27 eV, which means that this is not a bound state with respect to a desorbed hydrogen molecule. Instead, the forth molecule attaches as a molecule to one of the Pd atoms of the cluster with an adsorption energy of 0.51 eV. Almost degenerate in energy, although slightly more stable, 0.52 eV, is the configuration with two dissociated molecules and two non-dissociated adsorbed molecules. The succesive molecular adsorption of a fith and a sixth hydrogen molecules on the Pd_6 with three dissociated and one non-dissociated adsorbed hydrogen molecules takes place with adsorption energies of 0.52 eV and 0.42 eV, respectively. The adsorption energies drop dramatically down to 0.16 eV and 0.10 eV, and 0.09 eV, respectively, for the succesive adsorption of three more hydrogen molecules. These energies have little interest for the storage of hydrogen at room temperature. In summary, Pd_6 is able to chemisorb dissociatively up to three hydrogen molecules, and to adsorb, with reasonably high energies, three non-dissociated additional molecules. These results are summarized in the columns labelled as ICO of Table 2. The transition from stable dissociative chemisorption to the molecular adsorption takes place when all the favorable sites of the upper side of the bipyramid (faces and Pd–Pd bonds not in

direct contact with the graphene surface and not involving the Pd atom saturating the vacancy) have been filled. Notice that due to steric effects it is not possible to fill out all the favorable faces and edges. For instance, the adsorption of H atoms on two edges of a triangle prevents the adsorption of a H atom on the face.

For completeness, we have also studied the competition between dissociative and molecular adsorption on the octahedral structure, OCT, of the anchored Pd_6 cluster with one disocciatively chemisorbed hydrogen molecule. The dissociative channel is preferred for the adsorption of the second hydrogen molecule, with an adsorption energy of 0.81 eV, whereas the molecular adsortion energy is 0.78 eV. The third hydrogen molecule adsorbes on Pd_6 with similar energies of 0.65 eV and 0.62 eV for the dissociative and the molecular channels, respectively. In contrast to the ICO case, the forth molecule can dissociate on the octahedral Pd_6 cluster with three dissociated hydrogen molecules, but the adsorption energy is very small, 0.03 eV, with respect to the desorbed molecule. However the fourth molecule can attach as a non-dissociated molecule whith an energy of 0.56 eV. The fith and sixth hydrogen molecules can also attach as non-dissociated molecules with adsorption energies of 0.48 eV and 0.50 eV, respectively. A seventh molecule can not attach directly to the Pd cluster and begins to form a second layer at a larger distance and with a much lower adsorption energy. Those structures are shown in Fig.5 and the results are summarized in the columns labelled as OCT of Table 2.

From our results we conclude that the successive adsorption of hydrogen on Pd clusters anchored on graphene vacancies does not depend much on the structure of the Pd clusters, since a similar behaviour has been found for Pd_6 in the ICO and the OCT structures. Once the Pd cluster is saturated with dissociated hydrogen molecules, it is still able to adsorb more hydrogen following the molecular channel. Therefore, the Pd clusters anchored on graphene vacancies retain their capacity to adsorb hydrogen. Clearly, the number of adsorbed hydrogen molecules in the supported clusters is smaller than for free gas phase clusters[24] due to the steric effects of the graphene layer. However, gas phase clusters are not appropriate models for hydrogen storage or other material applications. Pd doping contributes to an enhancement of the amount of

Figure 4: Top and side views of successive adsorption of hydrogen on the ICO structure of anchored Pd_6 with one dissociatively chemisorbed hydrogen molecule. Both the molecular and the dissociative channels are shown from $n = 2$ to $n = 4$, and only the molecular channel is shown for $n = 5-9$. The adsorption energies of the last hydrogen molecule are calculated using Eq.1.

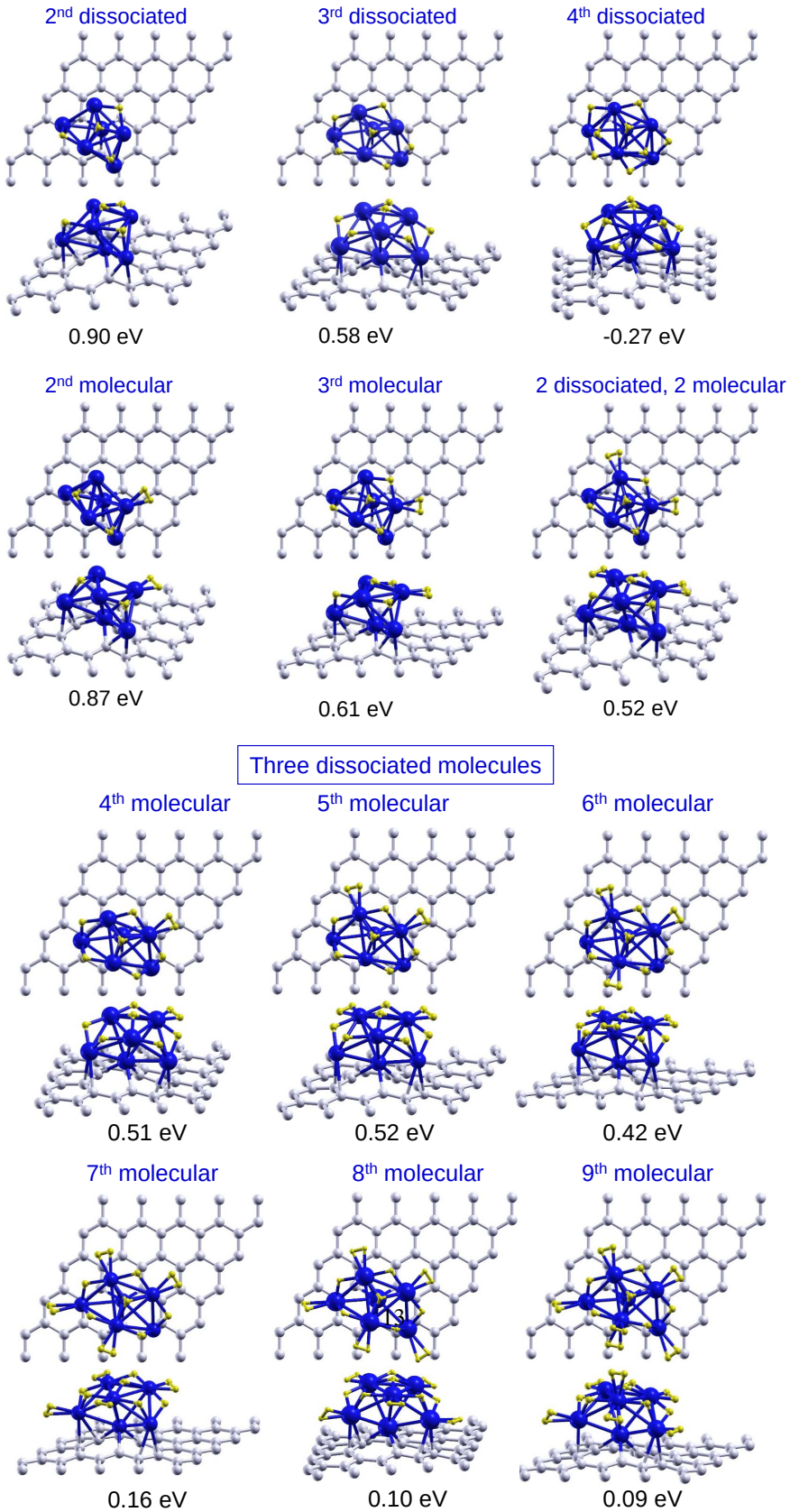

Figure 5: Top and side views of successive adsorption of hydrogen on the OCT structure of anchored Pd_6 with one disociatively chemisorbed hydrogen molecule. Both the molecular and the dissociative channels are shown from $n = 2$ to $n = 4$, and only the molecular channel is shown for $n = 5-7$. The adsorption energies of the last hydrogen molecule are calculated using Eq.1.

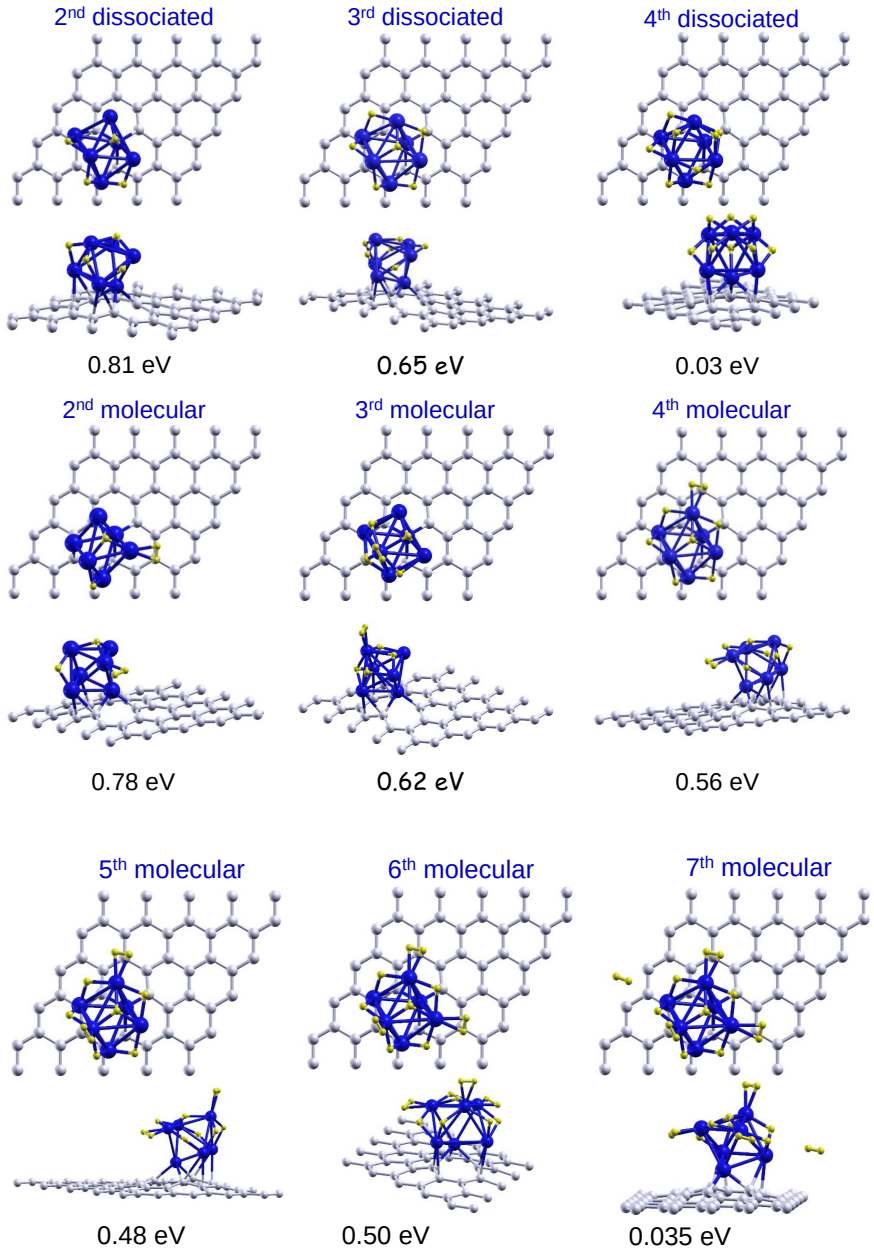

hydrogen stored in a Pd-doped porous carbon material.

On the other hand, the so-called spillover mechanism[25] has been proposed as the responsible of the enhancement. According to this mechanism, the molecules adsorbed on a first surface are transported to a second surface that does not adsorb the molecules under the same conditions. Our results on the adsorption and saturation with hydrogen of supported Pd clusters correspond to the first step of the spillover mechanism. The transfer mechanism of hydrogen attached to Pd towards the graphene layer, where the adsorption energies of hydrogen are less than 100 meV, remains to be elucidated. It is also interesting to notice that in order to use the stored hydrogen as a fuel, molecular hydrogen has to be catalytically dissociated in the anode of the hydrogen fuell cell. Palladium and other transition metals are usually employed as catalysts in this dissociation step. Our results on the dissociation of H_2 on supported palladium clusters provide a first hint on the role played by Pd clusters in the anode of the hydrogen fuell cells.

3.4 Bonding between hydrogen and the Pd cluster.

To investigate the nature of the bonding between hydrogen and the Pd cluster, both in the molecular and the dissociative channels, we have calculated the electronic density difference between the system with adsorbed hydrogen and the two separated subsystems, formed by the Pd cluster anchored to the graphene vacancy on one hand and the free hydrogen molecule or free hydrogen atoms, in the proper positions, on the other. Figure 6 shows the electronic density difference for the molecular adsorption of one, two and three hydrogen molecules on the OCT Pd_6. There is an increase (yellow surface in the figure) of electronic density in the region between the hydrogen molecule and the Pd atom to which the molecule is attached, what indicates a covalent-type of bonding between the hydrogen molecule and the Pd atom. Moreover, some polarization of the electronic density is also apparent. It is interesting to notice that the same type of bonding is observed for an increasing number of hydrogen molecules attached to different Pd atoms and also in the case of two hydrogen molecules attached to the same Pd atom. This indicates that the hydrogen molecules bind independently to the Pd cluster. The top panels of Figure 7 show the electronic density difference for the

Figure 6: Electronic density difference between the system with adsorbed hydrogen and the separated subsystems, formed by the Pd cluster anchored to the graphene vacancy on one hand and the free hydrogen molecule (in the proper position) on the other, for the molecular adsorption of $n = 1 - 3$ hydrogen molecules on the OCT structure of Pd_6. The yellow isosurfaces correspond to positive values of the electronic density difference and the green isosurfaces to negative values. Red, blue and grey balls represent H, Pd and C atoms, respectively.

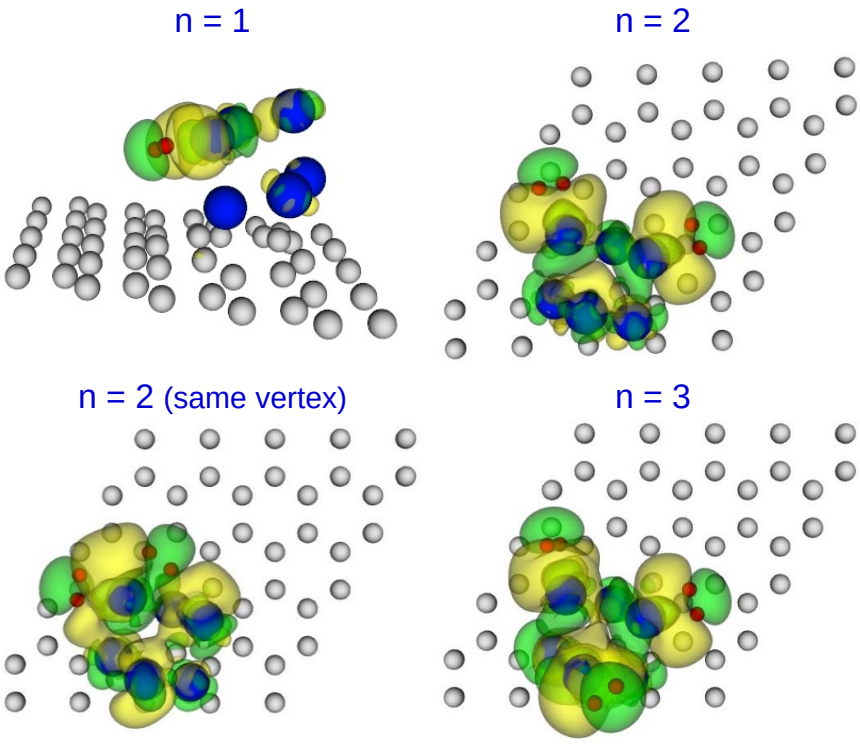

dissociative chemisorption of hydrogen on the ICO and the OCT structures of Pd_6. Here, each hydrogen atom is embedded in a region of positive electronic density difference, that is, each hydrogen builds up an excess of electronic density around it. This type of bonding is typical of metal hydrides and could be interpreted as an ionic type of bonding. A similar behaviour is found in the case of two disociatively chemisorbed hydrogen molecules on ICO Pd_6 (see lower left pannel of Fig.7). Both bonding types can be observed simultaneously in the case of two adsorbed hydrogen molecules, one dissociatively chemisorbed and the second adsorbed as a non-dissociated molecule (see lower right pannel of Fig.7). This indicates that the two adsorption channels take place

Figure 7: Electronic density difference between the system with adsorbed hydrogen and the separated subsystems formed by the Pd cluster anchored to the graphene vacancy on one hand and the free hydrogen atoms or the free molecule (in the proper position) on the other. Top panels stand for the dissociative chemisorption of one hydrogen molecule on the ICO (left) and the OCT (right) structure of Pd_6. The lower panels stand for the adsorption of two hydrogen molecules: in the left, the two molecules are chemisorbed; in the right, one molecule is chemisorbed and the other adsorbed as a non-dissociated molecule. Yellow isosurfaces correspond to positive values of the electronic density difference and green isosurfaces to negative values. Red, blue and grey balls represent H, Pd and C atoms, respectively.

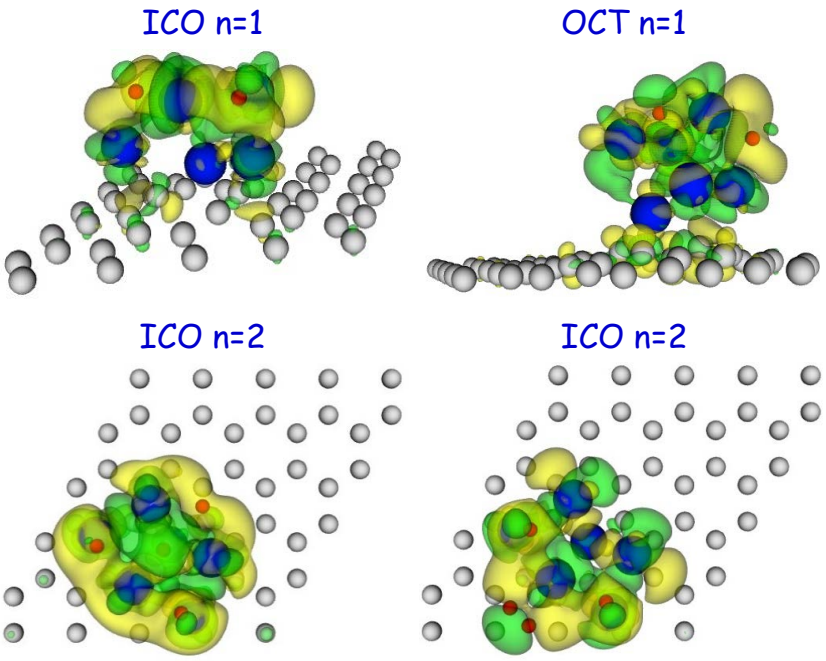

independently of each other, and do not involve the complete Pd cluster but involve locally the nearby Pd atoms only. It is also noticeable that the graphene layer does not participate actively on the adsorption of hydrogen on the anchored Pd clusters.

Since the adsorption and dissociation of hydrogen is mainly due to local interaccions with the palladium clusters, we expect similar adsorption and dissociation mechanisms on Pd clusters anchored on graphene vacancies and on Pd clusters deposited on pristine graphene. The hydrogen dissociation barriers in the latter are about 0.3 eV [15] and, therefore, similar values are expected for dissociation of hydrogen on Pd clusters anchored on graphene vacancies.

3.5 Desorption of hydrogen

Let us now focus on the desorption step of the hydrogen storage cycle. The desorption energy of hydrogen is equal to the adsorption energy. This energy is to be compared with the energy required to desorb the Pd_6-H_2 complexes for both the molecular adsorption and the dissociative chemisorption channels. The desorption energy of the Pd_6-H_2 complex from the graphene layer with a vacancy in the case of molecular adsorption on the OCT structure of Pd_6 is of 5.66 eV. Similar energies, 5.62 and 5.89 eV, are found for desorption of the Pd_6-H_2 complex when hydrogen is dissociativeley chemisorbed on the OCT and ICO structures of Pd_6, respectively. All those energies are much higher than the desorption energies of the H_2 molecule: 0.74 eV in the case of molecular adsorption on OCT Pd_6, and 1.03 and 1.25 eV for the cases of dissociative chemisorption on the OCT and ICO structures of Pd_6, respectively. Therefore in the desorption step of the storage cycle, only hydrogen will be released because the energies required to release Pd-H complexes are too high. This is in contrast with the desorption behaviour found for Pd clusters deposited on pristine graphene. There, the desorption energies of the Pd-H complexes are similar to the desorption energies of hydrogen molecules (roughly between 0.5 and 1 eV) and, therefore, desorption of complexes competes with the desorption of hydrogen, thus spoiling the beneficial effect of the Pd dopant on the storage capacity of the nanoporous carbon materials. Here, the Pd clusters are firmly anchored to a graphene vacancy (5.62 eV), what prevents the desorption of the Pd-H complexes. As a conclusion we find that anchoring Pd_6 to a graphene vacancy retains the capabilities of the cluster to adsorb hydrogen but completely inhibits the possibility of desorption of the Pd-H complexes. A similar behaviour was found for Pd atoms anchored on graphene vacancies. This solves the problem of desorption of Pd-H complexes that was present in the case of Pd atoms and clusters supported on pristine graphene.

4 Conclusions

Hydrogen adsorption on nanoporous carbon materials is one of the most promising technologies for hydrogen storage. In this paper we have investigated the adsorption, dissociation and desorption of hydrogen from Pd_6 clusters anchored on graphene vacancies, on the basis of the Density Functional Formalism. The graphene layer with a vacancy is used as a model of the defective pore walls of nanoporous carbons and the Pd_6 cluster is considered as a representative of small-size Pd clusters. The effect of vacancies on the hydrogen adsorption cannot be assessed from studies of Pd clusters supported on pristine graphene. Pd_6 anchored on a vacancy may attach directly up to six hydrogen molecules with adsorption energies in the range of 0.3 - 0.7 eV. Six adsorbed molecules saturate the cluster and, due to steric effects, additional hydrogen molecules cannot attach directly to the Pd cluster and will begin to form a second hydrogen shell at a larger distance from the cluster and very weakly bound to it. The dissociative chemisorption of hydrogen is preferred over the molecular adsorption for adsorption from one to three hydrogen molecules. The dissociative adsorption energies are in the range of 0.6-1.2 eV. The six atoms of three hydrogen molecules saturate all the favorable sites of the Pd cluster for chemisorption: the faces and Pd–Pd bonds not in direct contact with the graphene layer and not involving the Pd atom which saturates the graphene vacancy. However not all those faces and edges can be simultaneously filled due to steric effects. Three additional hydrogen molecules can be adsorbed as non-dissociated molecules onto Pd cluster with three chemisorbed molecules, with adsorption energies of 0.5 eV. The desorption of hydrogen will take place with desorption energies in the range of 0.3 - 1.2 eV. On the other hand, since the Pd cluster is firmly anchored to the graphene vacancy, desorption of Pd-H complexes requires much higer energies, by a factor of 5, than desorption of hydrogen. Then the desorption step of the storage cycle will involve only desorption of hydrogen. Therefore, anchoring the Pd clusters to vacancies is very promising because i) the anchored Pd clusters retain their capacity of adsorbing hydrogen, and ii) it completely prevents the desorption of Pd-H complexes, which was a problem in the case of Pd clusters supported on pristine

graphene. Our results on the dissociative adsorption channel are also of interest for the catalytic dissociation process in the anode of the hydrogen fuel cells.

Acknowledgments

This work was supported by MICINN of Spain (Grant MAT2011-22781) and Junta de Castilla y León (Grant VA050U14).

References

[1] DOE, *Multi-Year Research, Development and Demonstration Plan: Planned Program Activities for 2005-2015. Technical Plan–Storage. Updated April 2009*, http://www1.eere.energy.gov/hydrogenandfuelcells/mypp/pdfs/storage.pdf, 2009.

[2] P. Jena, *J. Phys. Chem. Lett.*, 2011, **2**, 206–211.

[3] Y. Gogotsi, R. K. Dash, G. Yushin, T. Yildirim, G. Laudisio and J. E. Fischer, *J. Am. Chem. Soc.*, 2005, **127**, 16006–7.

[4] A. Linares-Solano, M. Jordá-Beneyto, D. L.-C. M. Kunowsky, F. Suárez-García and D. Cazorla-Amorós, in *Carbon Materials: Theory and Practice*, ed. P. G. A.P. Terzyk and P. Kowalczyk, Research Signpost, Kerala, India, 2008, pp. 245–281.

[5] I. Cabria, M. J. López and J. A. Alonso, *Carbon*, 2007, **45**, 2649–2658.

[6] I. Cabria, M. J. López and J. A. Alonso, *Int. J. Hydrogen Energy*, 2011, **36**, 10748–10759.

[7] J. S. Arellano, L. M. Molina, A. Rubio and J. A. Alonso, *J. Chem. Phys.*, 2000, **112**, 8114–9.

[8] J. A. Alonso, J. S. Arellano, L. M. Molina, A. Rubio and M. J. López, *IEEE Trans. Nanotechnol.*, 2004, **3**, 304–310.

[9] B. K. Pradhan, G. U. Sumanasekera, K. W. Adu, H. E. Romero, K. A. Williams and P. C. Eklund, *Physica B*, 2002, **323**, 115–121.

[10] G. E. Froudakis, *J. Phys.-Condes. Matter*, 2002, **14**, R453.

[11] C. I. Contescu, K. van Benthem, S. Li, C. S. Bonifacio, S. J. Pennycook, P. Jena and N. C. Gallego, *Carbon*, 2011, **49**, 4050–4058.

[12] M. J. López, I. Cabria and J. A. Alonso, *J. Chem. Phys.*, 2011, **135**, 104706.1–9.

[13] I. López-Corral, E. Germán, M. A. Volpe, G. P. Brizuela and A. Juan, *Int. J. Hydrogen Energy*, 2010, **35**, 2377–2384.

[14] I. López-Corral, E. Germán, A. Juan, M. A. Volpe and G. P. Brizuela, *J. Phys. Chem. C*, 2011, **115**, 4315–4323.

[15] I. Cabria, M. J. López, S. Fraile and J. A. Alonso, *J. Phys. Chem. C*, 2012, **116**, 21179–21189.

[16] M. J. López, I. Cabria and J. A. Alonso, *J. Phys. Chem. C*, 2014, **118**, 5081–5090.

[17] I. López-Corral, J. D. Celis, A. Juan and B. Irigoyen, *Int. J. Hydrogen Energy*, 2012, **37**, 10156–10164.

[18] I. Cabria, M. J. López and J. A. Alonso, *Phys. Rev. B*, 2010, **81**, 035403.

[19] dacapo, *See https://wiki.fysik.dtu.dk/dacapo for a description of the total energy code, based on the density functional theory.*, 2009.

[20] D. Vanderbilt, *Phys. Rev. B*, 1990, **41**, R7892.

[21] H. Monkhorst and J. Pack, *Phys. Rev. B*, 1976, **13**, 5188–5192.

[22] J. P. Perdew and Y. Wang, *Phys. Rev. B*, 1992, **45**, 13244.

[23] I. Cabria, M. J. López and J. A. Alonso, *Comput. Mater. Sci.*, 2006, **35**, 238–42.

[24] C. Zhou, S. Yao, J. Wu, R. C. Forrey, L. Chen, A. Tachibana and H. Cheng, *Phys. Chem. Chem. Phys.*, 2008, **10**, 5445–5451.

[25] W. Conner and J. Falconer, *Chem. Rev.*, 1995, **95**, 759–788.

Table 1: Successive adsorption of hydrogen, in the molecular channel, on Pd_6 with octahedral structure anchored on a graphene vacancy. The star (*) indicates the most stable configuration of the molecular channel with a fixed number n of molecules adsorbed on the Pd_6 cluster. The adsorption energies are calculated from Eq. 1 where $E[(n-1)H_2 + Pd_6 \text{ on } G_{vac}]$ is the energy of the most stable configuration of the molecular channel with $n-1$ adsorbed molecules. The energies are given in eV

n	Different Vertices E_{ad}^{nth}	Two in same Vertex E_{ad}^{nth}
1	0.74*	
2	0.73*	0.44
3	0.53*	0.40
4	0.47	0.50*
5	0.34	0.36*
6		0.34*

Table 2: Adsorption energies of the successive adsorption of hydrogen on Pd_6 with ICO (OCT) structure anchored on a graphene vacancy. The nth molecule is adsorbed on previous ICO (OCT) configurations (structures with $n-1$ hydrogen molecules). For $n = 1$ the adsorption energy is calculated with respect to the most stable OCT structure of Pd_6 anchored on a graphene vacancy. The star (*) indicates the preferred adsorption channel for the nth molecule adsorbed on the icosahedral (octahedral) structure. Energies are given in eV.

n	ICO Dissociative Channel E_{ad}^{nth}	ICO Molecular Channel E_{ad}^{nth}	OCT Dissociative Channel E_{ad}^{nth}	OCT Molecular Channel E_{ad}^{nth}
	n dissociated	1 molecular	n dissociated	1 molecular
1	1.25*		1.03*	0.74
2	0.90*	0.87	0.81*	0.78
3	0.58	0.61*	0.65*	0.62
4	-0.27	0.51	0.03	0.56*
		(n-2) molecular		
4		0.52*		
		(n-3) molecular		(n-3) molecular
5		0.52*		0.48*
6		0.42*		0.50*
7		0.16*		
8		0.10*		
9		0.09*		